

## STRESS STATE IN THE VICINITY OF AN INCLINED ELLIPTICAL DEFECT AND STRESS INTENSITY FACTORS FOR BIAXIAL LOADING OF A PLATE

A. A. Ostsemin<sup>1</sup> and P. B. Utkin<sup>2</sup>

UDC 620.170.5; 539.4

*The problem of determining the stress state of a plate with an inclined elliptical notch under biaxial loading is considered. The Kolosov–Muskhelishvili method is used to obtain an expression for the stress near the vertex of an inclined ellipse, whose particular case are expressions for the stress in the case of an inclined crack. The stress intensity factors  $K_I$  and  $K_{II}$  were determined experimentally by holographic interferometry in the case of extension of a plate with an inclined crack-like defect. The calculation results are compared with experimental data.*

**Key words:** fracture mechanics, stress intensity factors, Kolosov–Muskhelishvili method, stress state, plate with an inclined elliptical notch, holographic interferometry.

**Introduction.** The fracture stress criteria can be classified as simple and complex. The simple criteria take into account only the singular stress component and are expressed in terms of stress intensity factors (SIFs). The complex criteria are obtained by a refined analysis of the stress state (SS) near the tip a crack-like defect and take into account the regular stress component [1]. In the case of slant cracks, a defect is modeled by an elliptical notch. The most widely used and best validated approach is the one in which the SS characteristics should be determined not at the crack tip but at a certain distance  $r_0$  from it [1, 2]. Holographic interferometric studies [3] using complex criteria of the limiting equilibrium of an inclined crack [1] have provided experimental data which are in better agreement with the results of theoretical studies [1]. The error was 4.7%.

Eftis and Subramonian [1] obtained a more exact expression for the Westergaard function contained in the singular solution for an inclined crack in a plate under biaxial loading [1]. This approximate two-component solution is fairly exact. Theocaris and Michopoulos [2] obtained an exact solution of the problem for the stress tensor in a plane with an inclined crack under biaxial loading using expressions for the complex potentials  $\Phi(z)$  and  $\Omega(z)$  [4]. The relative error of the sum  $\sigma_1 + \sigma_2$  and the difference  $\sigma_1 - \sigma_2$  in the principal stresses obtained using both methods was determined in [2]. The effect of the biaxial loading  $\varepsilon$  on the stress tensor components  $\sigma_x$ ,  $\sigma_y$ , and  $\tau_{xy}$  and the maximum shear stress  $\tau_{\max}$  has been studied using the Kolosov–Muskhelishvili method [4]. Theocaris and Spyropoulos [5] presented isochromatic patterns and gave a review of photoelasticity methods for a plate with an inclined crack. In the present paper, the results [2] for a plate with an elliptical notch are extended to the biaxial loading of the plate. Expressions for the stress tensor components are obtained, the effect of the ellipse parameter  $m$  for the biaxial loading of a plate with an inclined elliptical notch is studied, and experimental data obtained using holographic interferometry are given.

Methods of fracture mechanics allow one to determine the fracture resistance of metal welded joints in the presence of cracks. However, a feature of welded joints is that they contain stress concentrators (pores, lack of fusion, lack of penetration, undercuts, slag inclusions) with small radii  $\rho = 0.01\text{--}0.10$  mm, which can lead to fracture of the welded structures [6]. The direct use of the propositions of fracture mechanics to study the stress concentration characteristic of welded joints is incorrect [7].

---

<sup>1</sup>South Ural Research-and-Production Center, Chelyabinsk 450019. <sup>2</sup>South Ural State University, Chelyabinsk 454080; shum@math.susu.ac.ru. Translated from *Prikladnaya Mekhanika i Tekhnicheskaya Fizika*, Vol. 50, No. 1, pp. 118–127, January–February, 2009. Original article submitted September 21, 2007; revision submitted June 11, 2008.

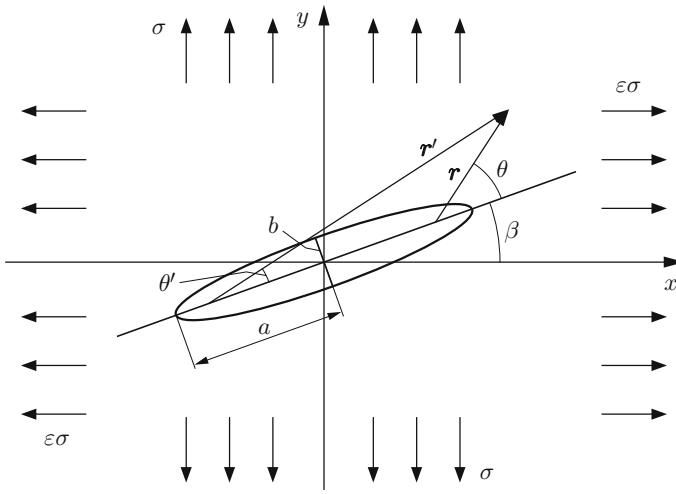


Fig. 1. Diagram of the problem of an inclined elliptical notch in a plate subjected to biaxial loading.

A review of the criteria, an analysis of their applicability to calculations of the limiting equilibrium and the growth trajectory of cracks oriented arbitrarily in the field of the stresses acting on the solid, and the values of the limiting radius  $\rho_0$  are given in [8].

The objective of the present paper is to theoretically determine the SS and SIFs in the case of an inclined elliptical notch in a plate under biaxial loading.

**1. Stress in the Case of an Elliptical Hole in a Plate under Biaxial Loading.** The stress state of a plate with an inclined elliptical notch subjected to biaxial loading is considered. A diagram of the problem is shown in Fig. 1. According to the Kolosov–Muskhelishvili formulas [4], the stress tensor components in plane problems of elasticity are linked by the relations [4]

$$\sigma_x + \sigma_y = 2(\varphi'(z) + \overline{\varphi'(z)}), \quad \sigma_y - \sigma_x + 2i\tau_{xy} = 2(\overline{z}\varphi''(z) + \psi'(z)) \quad (1.1)$$

( $z = x + iy$  is a complex variable).

The complex potentials  $\varphi(z)$  and  $\psi(z)$  are represented as the sum [4]

$$\varphi(z) = \Gamma z + \tilde{\varphi}(z), \quad \psi(z) = \Gamma' z + \tilde{\psi}(z), \quad (1.2)$$

where  $\Gamma = (1 + \varepsilon)\sigma/4$ ,  $\Gamma' = (1 - \varepsilon)\sigma e^{-2i\beta}/2$ ,  $\varepsilon$  is the biaxial loading parameter equal to the ratio of the principal stresses at infinity,  $\sigma$  is the nominal stress along the  $y$  axis, and  $\beta$  is the angle between the axis of the defect and the  $x$  axis corresponding to the first principal stresses (see Fig. 1). Definitions of the coefficients  $\Gamma$  and  $\Gamma'$  are presented in [4]. The functions  $\tilde{\varphi}$  and  $\tilde{\psi}$  are holomorphic in the vicinity of infinity, and  $\tilde{\varphi}$  is equal to zero at infinity.

Using a conformal change of coordinates, we convert to the new variable  $\zeta$  by means of the transformation

$$z = R(\zeta + m/\zeta) = \omega(\zeta). \quad (1.3)$$

The quantities  $R$  and  $m$  are the ellipse parameters and are linked to the lengths of the semiaxis  $a$  and  $b$  by the relations

$$R = \frac{a+b}{2}, \quad m = \frac{a-b}{a+b}.$$

This transformation converts part of the plane outside the ellipse into the plane outside the unit circle with center at the coordinate origin.

In view of (1.3), expressions (1.2) for the functions  $\varphi(z)$  and  $\psi(z)$  are written as

$$\varphi(\zeta) = \Gamma R \zeta + \left[ \Gamma \frac{Rm}{\zeta} + \tilde{\varphi}\left(R\left(\zeta + \frac{m}{\zeta}\right)\right) \right], \quad \psi(\zeta) = \Gamma' R \zeta + \left[ \Gamma' \frac{Rm}{\zeta} + \tilde{\psi}\left(R\left(\zeta + \frac{m}{\zeta}\right)\right) \right]. \quad (1.4)$$

Using the theory of residues and formulas (1.4) for the complex potentials, we obtain

$$\varphi(\zeta) = \Gamma R \left( \zeta - \frac{m}{\zeta} \right) - \frac{\overline{\Gamma'} R}{\zeta} = \frac{R\sigma}{4} \left[ (1 + \varepsilon) \left( \zeta - \frac{m}{\zeta} \right) - \frac{2(1 - \varepsilon) e^{2i\beta}}{\zeta} \right],$$

$$\begin{aligned}\psi(\zeta) &= \frac{R}{m} \left( m\Gamma' \zeta + \frac{\overline{\Gamma'}}{\zeta} \right) - \frac{(1+m^2)\zeta}{m(\zeta^2-m)} (2\Gamma R m + \overline{\Gamma'} R) \\ &= \frac{R\sigma}{2m} \left( (1-\varepsilon) \frac{m e^{-2i\beta} \zeta^2 + e^{2i\beta}}{\zeta} - ((1-\varepsilon) e^{2i\beta} + (1+\varepsilon)m)(1+m^2) \frac{\zeta}{\zeta^2-m} \right).\end{aligned}$$

In view of (1.3), the complex potentials  $\varphi(\zeta)$  and  $\psi(\zeta)$  are written as

$$\begin{aligned}\varphi(z) &= \frac{\sigma}{4m} \left\{ -(1-\varepsilon) e^{2i\beta} z + \left[ m(1+\varepsilon) + (1-\varepsilon) e^{2i\beta} \right] \sqrt{z^2-d^2} \right\}, \\ \psi(z) &= \frac{\sigma}{2} \left( (1-\varepsilon) \frac{e^{2i\beta} + e^{-2i\beta} m^2}{2m^2} z - (1-\varepsilon) \frac{e^{2i\beta} - e^{-2i\beta} m^2}{2m^2} \sqrt{z^2-d^2} \right. \\ &\quad \left. - \left[ m(1+\varepsilon) + (1-\varepsilon) e^{2i\beta} \right] \frac{1+m^2}{m(1+m)^2} \frac{a^2}{\sqrt{z^2-d^2}} \right)\end{aligned}$$

( $d$  is the focal length of the ellipse:  $d^2 = a^2 - b^2$ ).

To simplify the calculations, we use the complex functions  $\Phi(z) = \varphi'(z)$  and  $\Psi(z) = \psi'(z)$ , which are derivatives of the complex potentials  $\varphi(z)$  and  $\psi(z)$ :

$$\begin{aligned}\Phi(z) &= \frac{\sigma}{4m} \left( -(1-\varepsilon) e^{2i\beta} + \left[ m(1+\varepsilon) + (1-\varepsilon) e^{2i\beta} \right] \frac{z}{\sqrt{z^2-d^2}} \right), \\ \Psi(z) &= \frac{\sigma}{2} \left( (1-\varepsilon) \frac{e^{2i\beta} + e^{-2i\beta} m^2}{2m^2} - (1-\varepsilon) \frac{e^{2i\beta} - e^{-2i\beta} m^2}{2m^2} \frac{z}{\sqrt{z^2-d^2}} \right. \\ &\quad \left. + \left[ m(1+\varepsilon) + (1-\varepsilon) e^{2i\beta} \right] \frac{1+m^2}{m(1+m)^2} \frac{a^2 z}{(z^2-d^2)^{3/2}} \right).\end{aligned}\tag{1.5}$$

In the case of a central linear crack ( $m = 1$ ) for  $\beta = 0^\circ$ , the Westergaard function using expression (1.5) for the function  $\Phi(z)$  is written as

$$2\varphi'(z) = 2\Phi(z) = \frac{\sigma z}{\sqrt{z^2-a^2}} - \frac{1}{2}(1-\varepsilon)\sigma.$$

Earlier this expression was obtained in [1, 2].

To calculate the stress tensor, we use the formulas following from (1.1):

$$\begin{aligned}\sigma_x + \sigma_y &= 2(\Phi(z) + \overline{\Phi(z)}) = 4 \operatorname{Re}(\Phi(z)), & \sigma_x - \sigma_y &= 2 \operatorname{Re}(\overline{z}\Phi'(z) + \Psi(z)), \\ \tau_{xy} &= \operatorname{Im}(\overline{z}\Phi'(z) + \Psi(z)).\end{aligned}$$

To write the stress tensor components at the tip of the defect, we make the change of variables:

$$z = r e^{i\theta} + d = r' e^{i\theta'} - d, \quad 2d = r' e^{i\theta'} - r e^{i\theta}, \quad rr' = |z^2 - d^2|. \tag{1.6}$$

In view of (1.6), the complex potentials  $\Phi(z)$  and  $\Psi(z)$  can be written with the use of (1.5) as

$$\begin{aligned}\Phi(z) &= -A_0(\cos 2\beta + i \sin 2\beta) + (A_1 + iA_2) \frac{r \cos \theta + d + ir \sin \theta}{\sqrt{rr'}} \left( \cos \frac{\theta + \theta'}{2} - i \sin \frac{\theta + \theta'}{2} \right), \\ \Psi(z) &= A_0 \frac{1+m^2}{m} \cos 2\beta + i A_0 \frac{1-m^2}{m} \sin 2\beta \\ &\quad - A_0 \frac{r \cos \theta + d + ir \sin \theta}{\sqrt{rr'}} \left( \frac{1-m^2}{m} \cos 2\beta + i \frac{1+m^2}{m} \sin 2\beta \right) \left( \cos \frac{\theta + \theta'}{2} - i \sin \frac{\theta + \theta'}{2} \right) \\ &\quad + 2(A_1 + iA_2)a^2 B_1 \frac{r \cos \theta + d + ir \sin \theta}{(rr')^{3/2}} \left( \cos \frac{3(\theta + \theta')}{2} - i \sin \frac{3(\theta + \theta')}{2} \right),\end{aligned}\tag{1.7}$$

where

$$\begin{aligned} A_0 &= \frac{\sigma(1-\varepsilon)}{4m}, & A_1 &= \frac{\sigma[m(1+\varepsilon)+(1-\varepsilon)\cos 2\beta]}{4m}, \\ A_2 &= \frac{\sigma(1-\varepsilon)\sin 2\beta}{4m}, & B_1 &= \frac{1+m^2}{(1+m)^2}. \end{aligned}$$

The derivative of the complex potential  $\Phi'(z)$  is equal to

$$\Phi'(z) = -(A_1 + iA_2)a^2B_2 \frac{1}{(rr')^{3/2}} \left( \cos \frac{3(\theta+\theta')}{2} - i \sin \frac{3(\theta+\theta')}{2} \right), \quad (1.8)$$

where  $B_2 = d^2/a^2 = 4m/(1+m)^2$ .

Using (1.7) and (1.8), the expressions for the sum  $\sigma_x + \sigma_y$  and difference  $\sigma_x - \sigma_y$  of the normal stresses and the shear stress  $\tau_{xy}$  can be written as

$$\sigma_x + \sigma_y = 4A_1F_1 - 4A_0\cos 2\beta - 4A_2F_2; \quad (1.9)$$

$$\begin{aligned} \sigma_y - \sigma_x &= 2A_0 \frac{1+m^2}{m} \cos 2\beta + \frac{4a^2r\sin\theta}{(rr')^{3/2}} G_1 - 2A_0F_1 \frac{1-m^2}{m} \cos 2\beta \\ &\quad + 2A_0F_2 \frac{1+m^2}{m} \sin 2\beta + (r\cos\theta+d) \frac{4a^2}{(rr')^{3/2}} \frac{(1-m)^2}{(1+m)^2} G_2; \end{aligned} \quad (1.10)$$

$$\begin{aligned} \tau_{xy} &= A_0 \frac{1-m^2}{m} \sin 2\beta + 2r\sin\theta \frac{a^2}{(rr')^{3/2}} G_2 - A_0F_2 \frac{1-m^2}{m} \cos 2\beta \\ &\quad - A_0F_1 \frac{1+m^2}{m} \sin 2\beta - 2(r\cos\theta+d) \frac{a^2}{(rr')^{3/2}} \frac{(1-m)^2}{(1+m)^2} G_1. \end{aligned} \quad (1.11)$$

Here

$$\begin{aligned} F_1 &= \frac{1}{\sqrt{rr'}} \left( (r\cos\theta+d) \cos \frac{\theta+\theta'}{2} + r\sin\theta \sin \frac{\theta+\theta'}{2} \right), \\ F_2 &= \frac{1}{\sqrt{rr'}} \left( -(r\cos\theta+d) \sin \frac{\theta+\theta'}{2} + r\sin\theta \cos \frac{\theta+\theta'}{2} \right), \\ G_1 &= A_1 \sin \frac{3(\theta+\theta')}{2} - A_2 \cos \frac{3(\theta+\theta')}{2}, \quad G_2 = A_1 \cos \frac{3(\theta+\theta')}{2} + A_2 \sin \frac{3(\theta+\theta')}{2}. \end{aligned}$$

From relations (1.9) and (1.10), we obtain the stress tensor components  $\sigma_x$  and  $\sigma_y$ :

$$\begin{aligned} \sigma_x &= A_0 \cos 2\beta \left( -\frac{(1-m)^2}{m} - 4 \right) + \left( 2A_1 + A_0 \frac{1-m^2}{m} \cos 2\beta \right) F_1 + A_2 F_2 \left( -\frac{(1-m)^2}{m} - 4 \right) \\ &\quad - (r\cos\theta+d) \frac{2a^2}{(rr')^{3/2}} \frac{(1-m)^2}{(1+m)^2} G_2 - r\sin\theta \frac{2a^2}{(rr')^{3/2}} G_1, \\ \sigma_y &= A_0 \frac{(1-m)^2}{m} \cos 2\beta + \left( 2A_1 - A_0 \frac{1-m^2}{m} \cos 2\beta \right) F_1 + A_2 F_2 \frac{(1-m)^2}{m} \\ &\quad + (r\cos\theta+d) \frac{2a^2}{(rr')^{3/2}} \frac{(1-m)^2}{(1+m)^2} G_2 + r\sin\theta \frac{2a^2}{(rr')^{3/2}} G_1. \end{aligned} \quad (1.12)$$

From (1.6) it follows that

$$r'\cos\theta' = 2d + r\cos\theta, \quad r'\sin\theta' = r\sin\theta.$$

Thus, the coordinates  $r'$  and  $\theta'$  are expressed in terms of  $r$  and  $\theta$ , and formulas (1.11) and (1.12) depend only on  $r$  and  $\theta$ .

In the case of cracks for  $m = 1$ , relations (1.11) and (1.12) correspond to the expressions for the stress given in [2].

**2. Stress Intensity Factors in the Case of an Inclined Crack-Like Defect under Biaxial Loading.** Using the algorithm of [9, 10] and relation (1.5) for  $\Phi(z)$ , we determine the stress intensity factors:

$$K = K_I - iK_{II} = \lim_{z \rightarrow d} (2\sqrt{2\pi}\sqrt{z-d}\Phi(z)). \quad (2.1)$$

Transforming (2.1) and separating the real and imaginary parts, we obtain

$$K_I = \sqrt[4]{\frac{4m}{(1+m)^2}} \left( \sqrt{\pi a} \frac{\sigma(m(1+\varepsilon) + (1-\varepsilon)\cos 2\beta)}{2m} \right); \quad (2.2)$$

$$K_{II} = -\sqrt[4]{\frac{4m}{(1+m)^2}} \left( \sqrt{\pi a} \frac{\sigma(1-\varepsilon)\sin 2\beta}{2m} \right). \quad (2.3)$$

Hence,

$$A_1 = \frac{K_I}{2\sqrt{\pi a}} \sqrt[4]{\frac{(1+m)^2}{4m}} = \frac{K_I}{2\sqrt{\pi d}}, \quad A_2 = -\frac{K_{II}}{2\sqrt{\pi a}} \sqrt[4]{\frac{(1+m)^2}{4m}} = -\frac{K_{II}}{2\sqrt{\pi d}}. \quad (2.4)$$

Using (2.4), (1.11), and (1.12), the expressions for the stress tensor components  $\sigma_x$ ,  $\sigma_y$ , and  $\tau_{xy}$  are written as

$$\begin{aligned} \sigma_x &= A_0 \cos 2\beta \left( \frac{(1-m)^2}{m} - 4 + \frac{1-m^2}{m} F_1 \right) \\ &+ \frac{K_I}{2\sqrt{\pi a}} \sqrt[4]{\frac{(1+m)^2}{4m}} \left( 2F_1 - \cos \frac{3(\theta+\theta')}{2} (r \cos \theta + d) \frac{2a^2}{(rr')^{3/2}} \frac{(1-m)^2}{(1+m)^2} c - \sin \frac{3(\theta+\theta')}{2} r \sin \theta \frac{2a^2}{(rr')^{3/2}} \right) \\ &- \frac{K_{II}}{2\sqrt{\pi a}} \sqrt[4]{\frac{(1+m)^2}{4m}} \left[ \left( \frac{(1-m)^2}{m} - 4 \right) F_2 - \sin \frac{3(\theta+\theta')}{2} (r \cos \theta + d) \frac{2a^2}{(rr')^{3/2}} \frac{(1-m)^2}{(1+m)^2} + \cos \frac{3(\theta+\theta')}{2} r \sin \theta \frac{2a^2}{(rr')^{3/2}} \right], \\ \sigma_y &= A_0 \cos 2\beta \left( \frac{(1-m)^2}{m} - \frac{1-m^2}{m} F_1 \right) \\ &+ \frac{K_I}{2\sqrt{\pi a}} \sqrt[4]{\frac{(1+m)^2}{4m}} \left( 2F_1 + \cos \frac{3(\theta+\theta')}{2} (r \cos \theta + d) \frac{2a^2}{(rr')^{3/2}} \frac{(1-m)^2}{(1+m)^2} + \sin \frac{3(\theta+\theta')}{2} r \sin \theta \frac{2a^2}{(rr')^{3/2}} \right) \\ &- \frac{K_{II}}{2\sqrt{\pi a}} \sqrt[4]{\frac{(1+m)^2}{4m}} \left( \frac{(1-m)^2}{m} F_2 + \sin \frac{3(\theta+\theta')}{2} (r \cos \theta + d) \frac{2a^2}{(rr')^{3/2}} \frac{(1-m)^2}{(1+m)^2} - \cos \frac{3(\theta+\theta')}{2} r \sin \theta \frac{2a^2}{(rr')^{3/2}} \right), \\ \tau_{xy} &= -A_0 \cos 2\beta \frac{1-m^2}{m} F_2 \\ &- \frac{K_I}{2\sqrt{\pi a}} \sqrt[4]{\frac{(1+m)^2}{4m}} \left( \sin \frac{3(\theta+\theta')}{2} (r \cos \theta + d) \frac{2a^2}{(rr')^{3/2}} \frac{(1-m)^2}{(1+m)^2} - \cos \frac{3(\theta+\theta')}{2} 2r \sin \theta \frac{a^2}{(rr')^{3/2}} \right) \\ &- \frac{K_{II}}{2\sqrt{\pi a}} \sqrt[4]{\frac{(1+m)^2}{4m}} \left( \cos \frac{3(\theta+\theta')}{2} (r \cos \theta + d) \frac{2a^2}{(rr')^{3/2}} \frac{(1-m)^2}{(1+m)^2} \right. \\ &\left. + \sin \frac{3(\theta+\theta')}{2} r \sin \theta \frac{2a^2}{(rr')^{3/2}} + \frac{1-m^2}{m} - \frac{1+m^2}{m} F_1 \right). \end{aligned} \quad (2.5)$$

Expressions (2.5) for the stress tensor components  $\sigma_x$ ,  $\sigma_y$ , and  $\tau_{xy}$  differ from the formulas given in [2] in that they contain new additional terms with the elliptical notch parameter  $m$ . In the case of a crack, these terms vanish, resulting in the Theocaris solution [2].

**3. Experimental Determination of the SIFs  $K_I$  and  $K_{II}$  for an Inclined Elliptical Notch Using Holographic Interferometry.** A review of methods for determining the factors  $K_I$  and  $K_{II}$  on optically sensitive

plates with an inclined crack under uniaxial extension using photoelasticity and holographic Interferometry methods is given in [3, 5]. According to Neumann's theory and Hook's law and considering the deformations small, for a thin plate we have the following relationship between the fringe numbers  $N_1$  and  $N_2$  in patterns of absolute path differences (APD) and the principal stresses  $\sigma_1$  and  $\sigma_2$  [11]:

$$N_1 = a_1\sigma_1 + b_1\sigma_2, \quad N_2 = b_1\sigma_1 + a_1\sigma_2.$$

Here  $a_1 = 0.625$  fringe/MPa and  $b_1 = 0.453$  fringe/MPa are optical constants of the ED-20MPGFA material determined in a calibration experiment [12]. The polarization angle is reckoned from the vertical axis. In [12], a description is given of a calibrating procedure for photoelastic materials that increases the accuracy of determining the constants  $a_1$  and  $b_1$  by using all interference fringes observed and eliminating the interpolation operation in determining fringe numbers. The factors  $a_1$  and  $b_1$  were determined from the minimum condition for the standard deviation of their values obtained using experimental and theoretical fringes. The procedure [12] reduced the error of stress measurements from 26 to 12% at the same accuracy of processing of fringe patterns.

It is more convenient to process APD patterns along the axis of the crack-like defect (the largest number of fringes) for  $\theta = 0$  and  $\theta' = 0$ . Using the expression for the sum of the principal stresses  $\sigma_x + \sigma_y = \sigma_1 + \sigma_2$ , from (1.9), we obtain

$$\sigma_1 + \sigma_2 = \frac{N_1 + N_2}{a_1 + b_1} = -4A_0 \cos 2\beta + 4A_1 \frac{r + d}{\sqrt{r(r + 2d)}}. \quad (3.1)$$

Substitution of the first relation (2.4) into expression (3.1) yields

$$K_I^i = \sqrt{\pi d} \left( \frac{N_{1i} + N_{2i}}{a_1 + b_1} + \frac{\sigma(1 - \varepsilon)}{m} \cos(2\beta) \right) \frac{\sqrt{r_i(r_i + 2d)}}{2(r_i + d)}. \quad (3.2)$$

Using relation (1.10) for the difference of the normal stresses  $\sigma_x - \sigma_y$ , relation (1.11) for the shear stress  $\tau_{xy}$ , and the formula for the maximum shear stress  $4\tau_{\max}^2 = (\sigma_y - \sigma_x)^2 + 4\tau_{xy}^2$ , we obtain the following relation between the difference of the fringe numbers  $N_1 - N_2$  and the factors  $K_I$  and  $K_{II}$ :

$$\begin{aligned} (\sigma_1^i - \sigma_2^i)^2 &= \left( \frac{N_{1i} - N_{2i}}{a_1 - b_1} \right)^2 \\ &= \left( 2A_0 \frac{1+m^2}{m} \cos 2\beta - 2A_0 \frac{1-m^2}{m} \cos 2\beta \frac{r_i + d}{\sqrt{rr'}} + (r_i + d) \frac{4a^2}{(r_i r')^{3/2}} \frac{(1-m)^2}{(1+m)^2} \frac{K_I^i}{2\sqrt{\pi d}} \right)^2 \\ &\quad + 4 \left[ \frac{K_{II}^i}{2\sqrt{\pi d}} \left( 2(r_i + d) \frac{a^2}{(r_i r')^{3/2}} \frac{(1-m)^2}{(1+m)^2} + \frac{1-m^2}{m} - \frac{1+m^2}{m} \frac{r_i + d}{\sqrt{r_i r'}} \right) \right]^2. \end{aligned} \quad (3.3)$$

Here  $r' = r + 2d$  and  $\sigma_1^i$  and  $\sigma_2^i$  are the principal stresses on the notch axis at a distance  $r_i$  from the focus of the ellipse.

Using expression (3.2) for  $K_I$ , from Eq. (3.3) we obtain the relations for  $K_{II}$ :

$$K_{II}^i = \frac{1}{|D|} \sqrt{\left( \frac{N_{1i} - N_{2i}}{a_1 - b_1} \right)^2 - C^2}. \quad (3.4)$$

Here

$$\begin{aligned} C &= \frac{\sigma(1 - \varepsilon)}{2m} \cos 2\beta \left( \frac{1+m^2}{m} - \frac{1-m^2}{m} \frac{r_i + d}{\sqrt{r_i(r_i + 2d)}} \right) \\ &\quad + (r_i + d) \frac{4a^2}{(r_i(r_i + 2d))^{3/2}} \frac{(1-m)^2}{(1+m)^2} \frac{K_I^i}{2\sqrt{\pi d}}, \\ D &= \frac{1}{\sqrt{\pi d}} \left( 2(r_i + d) \frac{a^2}{(r_i(r_i + 2d))^{3/2}} \frac{(1-m)^2}{(1+m)^2} + \frac{1-m^2}{m} - \frac{1+m^2}{m} \frac{r_i + d}{\sqrt{r_i(r_i + 2d)}} \right). \end{aligned}$$

Experimental verification of theoretical formulas (3.2) and (3.4) for the stress intensity factors  $K_I$  and  $K_{II}$  was performed using the results of holographic interferometry studies [3, 13]. A plate with an inclined elliptical notch was subjected to uniaxial extension (defect length  $2a = 13.4$  mm, defect width  $b = 0.1$  mm, defect inclination

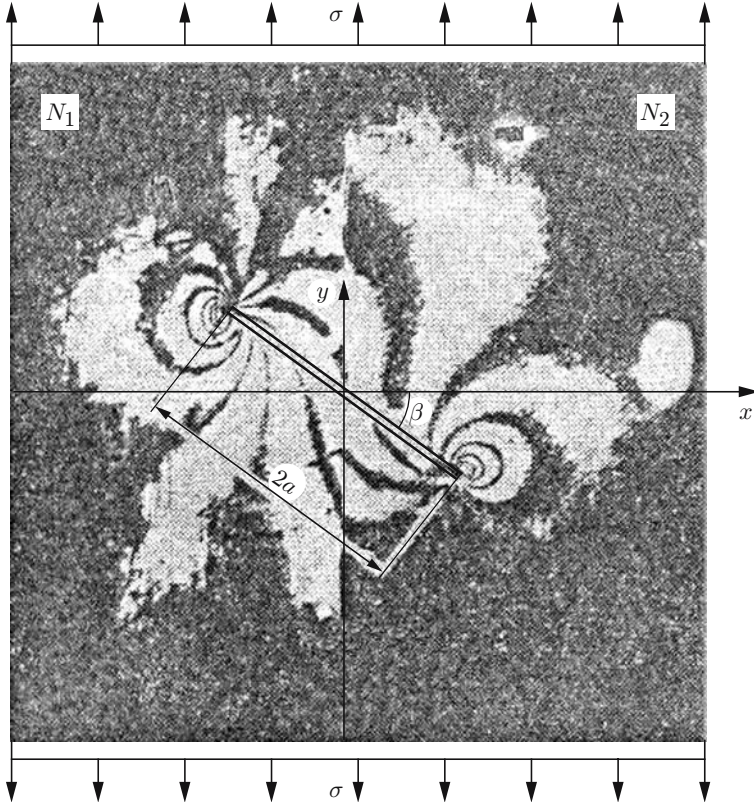


Fig. 2. Interference APD patterns for vertical and horizontal polarizations of the reference beam.

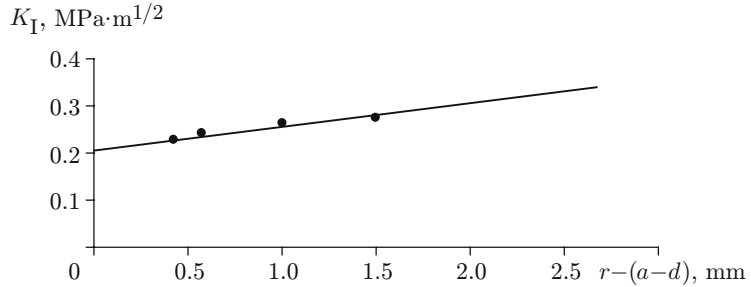


Fig. 3. Experimental dependence of the stress intensity factor  $K_I$  on the parameter  $r - (a - d)$  obtained by holographic interferometry.

angle  $\beta = 32.5^\circ$ , nominal stress  $\sigma = 2.1$  MPa, and plate width 96 mm). APD patterns were recorded using focused-image holograms. APD patterns (Fig. 2) were obtained by the two-exposure method. An LG-38 laser was used as a light source. The optical device and a description of the experiment are given in [14].

The SIF determination procedure makes it possible to construct plots of the fringe numbers  $N_1$  and  $N_2$  along the ellipse axis by APD patterns [15], to determine the values of  $N_{1i}$  and  $N_{2i}$  at the points  $r_i$ , to calculate  $K_I^i$  by expression (3.2), and to construct a plot of the relation  $K_I = K_I(r_i)$  with subsequent extrapolation to the vertex of the ellipse. From the sum of the fringe numbers of APD patterns  $N_1 + N_2$  using (3.2), we determined the stress intensity factor  $K_I$  and constructed a plot of  $K_I$  versus the distance  $r_i - (a - d)$  from the notch cut; the parameters  $a$  and  $d$  were determined from the length and width of the crack. Experimental values of  $K_I$  are approximated by an inclined straight line (Fig. 3). A similar approach was employed in [13, 16].

The results obtained were used to calculate the value  $K_I^{\text{exp}} = 0.211$  MPa·m<sup>1/2</sup> according to expression (3.2). This experimental value of  $K_I^{\text{exp}}$  agrees with the value of  $K_I^{\text{exp}} = 0.217$  MPa·m<sup>1/2</sup> calculated by formula (2.2) with

an error approximately equal to 2.7% for  $m = 0.97$ . The experimental value of  $K_{II}^{\exp} = 0.139 \text{ MPa} \cdot \text{m}^{1/2}$  calculated by formula (3.4) agrees with the value  $K_{II}^{\text{calc}} = 0.142 \text{ MPa} \cdot \text{m}^{1/2}$  calculated by expression (2.3) with an error equal to 2.1%.

The results indicate that the proposed procedure with an analysis of the APD fringe pattern at the tip of an elliptical notch provide high accuracy in determining SIFs.

In estimating the brittle fracture resistance of welds in the presence of inclined technological defects (lack of fusion, slag inclusions, lack of penetration), it is necessary to take into account the effect of the defect tip radius and the geometrical dimensions of the defect to determine the criterial characteristics of  $K_{Ic}$  and the stress intensity factors  $K_I$ .

**Conclusions.** The Kolosov–Muskhelishvili method was used to derive formulas for the stress tensor components at the tip of an elliptical notch, which, in a particular case, are degenerated into the relations for a linear crack [2].

In the case of an inclined elliptical notch, the experimental values of  $K_{Ic}$  determined by holographic interferometry agree with the calculated values with an error equal to 2.7%, and the value of  $K_I$  with an error equal to 2.1%.

## REFERENCES

1. J. Eftis and N. Subramonian, “The inclined crack under biaxial load,” *Eng. Fracture Mech.*, **10**, No. 1, 43–67 (1978).
2. P. S. Theocaris and J. G. Michopoulos, “A closed form solution of slant crack under biaxial loading,” *Eng. Fracture Mech.*, **17**, No. 2, 97–123 (1983).
3. A. A. Ostsemin, “Two-parametric determination of the stress intensity factors for an inclined crack using holographic interferometry,” *Zavod. Lab.*, No. 12, 45–48 (1991).
4. N. I. Muskhelishvili, *Some Primary Problems of the Mathematical Theory of Elasticity* [in Russian], Nauka, Moscow (1966).
5. P. S. Theocaris and C. P. Spyropoulos, “Photoelastic determination of complex stress intensity factors for slant crack under biaxial loading with higher-order term effects,” *Acta Mech.*, **48**, 57–70 (1983).
6. V. A. Vinokurov, *Welded Structures. Fracture Mechanics and Working Capacity Criteria* [in Russian], Mashinosstroenie, Moscow (1996).
7. V. A. Vinokurov, “Using the propositions of fracture mechanics to estimate the properties of welded joints,” *Svaroch. Proizv.*, No. 5, 2–4 (1977).
8. V. V. Panasyuk, *Mechanics of Quasibrittle Fracture of Materials* [in Russian], Naukova Dumka, Kiev (1991).
9. G. C. Sih and H. Liebowitz, “Mathematical theories of brittle fracture,” in: H. Liebowitz (ed.), *Fracture: An Advanced Treatise*, Vol. 2, Academic Press, New York (1968).
10. P. C. Paris and G. C. Sih, “Stress analysis of cracks,” in: *Fracture Toughness Testing and Its Applications*, Teck. Pub. 381, ASTM, Phil. Pa. 1965.
11. A. Ya. Aleksandrov and M. Kh. Akhmetzyanov, *Polarization Optical Methods of Deformable Solid Mechanics* [in Russian], Nauka, Moscow (1973).
12. A. A. Ostsemin, S. A. Deniskin, L. L. Sitnikov, et al., “Determining the stress state of solids with defects using holographic photoelasticity,” *Probl. Prochn.*, No. 10, 77–81 (1982).
13. A. A. Ostsemin, S. A. Deniskin, L. L. Sitnikov, et al. “Determining the stress intensity factors for an inclined crack using holographic interferometry,” *Zavod. Lab.*, No. 12, 66–69 (1987).
14. L. L. Sitnikov, A. A. Ostsemin, S. A. Deniskin, et al., “Determining the stress intensity factor  $K_I$  using holographic photoelasticity,” *Zavod. Lab.*, No. 9, 81–83 (1982).
15. A. A. Ostsemin, S. A. Deniskin, L. L. Sitnikov, et al. “Determining the stress intensity factor using photoelastic modeling methods,” *Probl. Prochn.*, No. 1, 33–37 (1990).
16. D. Broek, *Elementary Engineering Fracture Mechanics*, Martinus Nijhof Pub., Boston (1982).